Available online at www.sciencedirect.com
ScienceDirect
Biochimica et Biophysica Acta 1758 (2006) 1777–1786
BIOCHIMICA ET BIOPHYSICA ACTA
BBA
www.elsevier.com/locate/bbamem

Binding assays of inhibitors towards selected V-ATPase domains

F. Fernandes [a], L.M.S. Loura [a,b,*], A. Fedorov [a], N. Dixon [c], T.P. Kee [c], M. Prieto [a], M.A. Hemminga [d]

[a] *Centro de Química-Física Molecular, Instituto Superior Técnico, Lisbon, Portugal*
[b] *Departamento de Química, Universidade de Évora, Évora, Portugal*
[c] *Department of Chemistry, University of Leeds, Leeds LS2 9JT, UK*
[d] *Laboratory of Biophysics, Wageningen University, Wageningen, The Netherlands*

Received 14 March 2006; received in revised form 4 May 2006; accepted 13 July 2006
Available online 21 July 2006

Abstract

The macrolide antibiotic bafilomycin and the related synthetic compound SB 242784 are potent inhibitors of the vacuolar H^+-ATPases (V-ATPase). It is currently believed that the site of action of these inhibitors is located on the membrane bound c-subunits of V-ATPases. To address the identification of the critical inhibitors binding domain, their specific binding to a synthetic peptide corresponding to the putative 4th transmembrane segment of the c-subunit was investigated using fluorescence resonance energy transfer (FRET), and for this purpose a specific formalism was derived. Another peptide of the corresponding domain of the c′ isoform, was checked for binding of bafilomycin, since it is not clear if V-ATPase inhibition can also be achieved by interaction of the inhibitor with the c′-subunit. It was concluded that bafilomycin binds to the selected peptides, whereas SB 242784 was unable to interact, and in addition for bafilomycin, its interaction with the peptides either corresponding to the c- or the c′-subunit isoforms is identical. Since the observed interactions are however much weaker as compared to the very efficient binding of both bafilomycin and SB 242784 to the whole protein, it can be concluded that assembly of all V-ATPase transmembrane segments is required for an efficient interaction.

Keywords: V-ATPase; Bafilomycin A_1; Fluorescence; FRET

1. Introduction

Vacuolar ATPases (V-ATPases) are responsible for proton pumping in acidic organelles and plasma membranes of eukaryotic cells and their activity is essential in a large variety of cellular processes [1,2]. V-ATPases are composed of two domains (Fig. 1A), a soluble domain (V_1), where the catalytic center for ATP hydrolysis is located, and a membrane bound domain (V_0), responsible for proton pumping. V_0 contains multiple subunits including the 16-kDa proteolipids (subunits c) (4–5 copies) and their isoforms c′ and c″ (one copy each) [3], expected to play a major role in proton translocation. The c-subunit contains 4 putative transmembrane domains, and an essential glutamate residue located in the 4th putative transmembrane sequence is expected to be the carrier of protons across the membrane through protonation/deprotonation events [4].

Through site-directed mutagenic studies it was reported that mutations in three residues of the c-subunit of the V-ATPase from *Neurospora crassa* conferred resistance to bafilomycin A_1 (Fig. 1B) [5], a macrolide antibiotic inhibitor of V-ATPases produced by *Streptomyces griseus* [6]. Two of these residues reside in the same side of the putative 4th transmembrane helix (F136 and Y143), and this helix side is exposed to the lipid environment [7]. Immobilization of spin-labeled residues of c-subunit by concanamycin A, a macrolide antibiotic very similar in structure to bafilomycin A_1, has also been observed [8]. Also recently, six other sites where mutations induced resistance to bafilomycin A_1 were reported, and three of these are located in

* Corresponding author. Centro de Química-Física Molecular, Complexo I, Instituto Superior Técnico, Lisbon, Portugal.
E-mail address: pclloura@alfa.ist.utl.pt (L.M.S. Loura).

0005-2736/$ - see front matter © 2006 Elsevier B.V. All rights reserved.
doi:10.1016/j.bbamem.2006.07.006

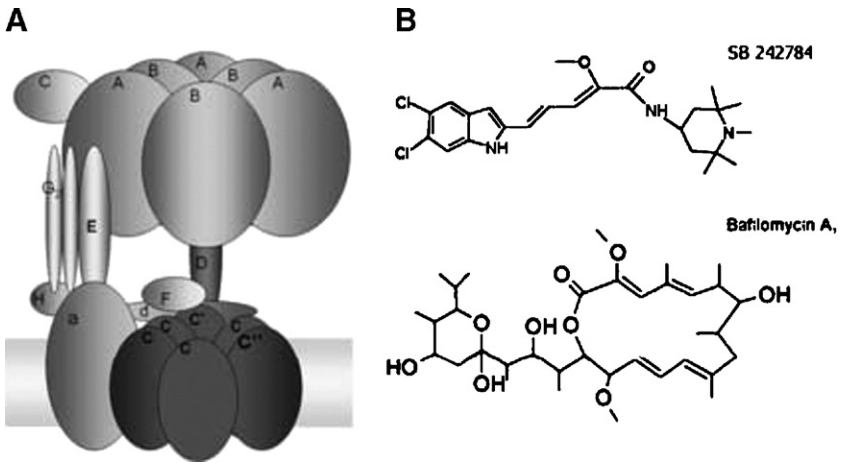

Fig. 1. (A) V-ATPase structure (adapted from [2]). (B) V-ATPase inhibitors SB 242784 and bafilomycin A_1.

the putative 4th transmembrane segment of c-subunit [9]. Of the latter, two residues are located in the same helix side as F136 and Y143, pointing to the existence of an inhibitor binding site on this protein surface. It is not clear yet if residues from other helices (1 and 2) could also be part of this binding site and form a binding pocket [9], as this structure would imply a different helix organization than the one suggested from cysteine cross-linking experiments [10].

The exact location and structure of the inhibitor binding site remains a matter of discussion, and in the present study we aim to detect the molecular requirements for bafilomycin A_1 binding through the use of a reductionist approach, using a simpler model system, a synthetic c-subunit derived peptide expected to mimic the putative 4th transmembrane segment of the V-ATPase c-subunit (Fig. 2). Synthetic peptides have proven to be useful tools in the characterization of ligand binding-sites on proteins and in some cases these isolated peptides were capable of ligand binding efficiencies identical to the intact protein [11–16]. Additionally, peptide fragments corresponding to transmembrane sequences in intact membrane proteins were shown to specifically disrupt the intact protein activity (likely by competing with native transmembrane domains) [17], and functional membrane proteins have already been reformed from reconstituted isolated transmembrane segments [18–20], proving that isolated peptides corresponding to transmembrane fragments are able to maintain specific information even when incorporated in the absence of its neighboring transmembrane segments. Similar to a previous study on synthetic peptides that mimic the 7th putative helix of the Vph1p subunit of yeast V-ATPase [21], flanking lysines were included in the design of the model peptides used in the present study to stabilize the transmembrane orientation due to the anchoring effect of the lysine residue.

H4	KKILILIFAEVLGLYGLIVALLLKK
$H4_{A\leftarrow E}$	KKILILIFAAVLGLYGLIVALLLKK
$H4_{c'}$	KKVLILIFSEVLGLYGMIVALILKK

Fig. 2. Primary sequence of the model peptides. The sequences correspond to the putative 4th transmembrane segment of the V-ATPase c-(H4) and c′-($H4_{c'}$) subunit from *Saccharomyces cerevisiae*. Peptide $H4_{A\leftarrow E}$ corresponds to a modification of peptide H4 in which the glutamate residue was replaced by an alanine. This mutation is underlined. The peptides were flanked by lysines to increase the membrane anchoring.

Another V-ATPase inhibitor, (2Z,4E)-5-(5,6-dichloro-2-indolyl)-2-methoxy-*N*-(1,2,2,6,6-pentamethylpiperidin-4-yl)-2,4-pentadienamide (SB 242784) (Fig. 1B), a synthetic molecule developed by Farina and coworkers [22] which is based on the presumptive pharmacophore of bafilomycin A_1 [23], and whose mechanism of inhibition is therefore expected to be similar, was proposed as an agent for a new therapeutical strategy in osteoporosis disease due to its specificity for the osteoclastic form of the enzyme [22,24]. Bafilomycines are powerful toxins, since they do not present specificity for any particular type of V-ATPases, inhibiting indiscriminately all enzymes, and thus preventing their therapeutical use. The reason for the difference in selectivity between the two inhibitors is still unclear, especially when noting that the inhibitor acts on the c-subunit that is extremely conserved between c-subunits from enzymes of different origins. A possible explanation would be the participation of the a-subunit (part of the enzyme membrane bound domain—V_0) (Fig. 1A) in the inhibitory mechanism, since the isoform a3 is expressed primarily in osteoclasts [25], and recent mutational studies support this hypothesis [26]. However, in a recent study using fluorescence resonance energy transfer (FRET), it was reported that SB 242784 and concanamycin bound competitively to isolated c-subunits, and SB 242784 was shown to bind to these as strongly as to the entire V_0 domain, apparently excluding a contribution of the a-subunit to the inhibitor binding mechanism [27]. The same authors also detected binding efficiencies of c-subunit for SB 242784 consistent with the inhibitor′s IC_{50} values, whereas for concanamycin these were slightly lower than expected [27]. Mutation of the tyrosine residue (Y143) from the 4th putative transmembrane segment had different effects on the conferred degree of resistance of yeast to concanamycin and to SB 242784, even though both were

increased [8]. The binding sites for both inhibitors seem, for this reason, to be overlapping but not identical.

Subunits c and c′ present a very large degree of sequence similarity, but mutations in subunit c′ homologous to those in subunit c producing bafilomycin A_1 insensitive strains have no effect in bafilomycin resistance [9]. On the basis of these results, Bowman and coworkers suggested that if c-subunit isoforms possess bafilomycin-binding sites, then these should have lower inhibitor affinities than in the c-subunit.

Using the UV absorption properties of bafilomycin A_1 (acceptor), we applied FRET in an assay (Tyr is the donor) to check for the existence of binding between the inhibitor and synthetic peptides corresponding to the putative 4th transmembrane segment of the c and c′-subunits from the V-ATPase of *Saccharomyces cerevisiae* in a lipidic environment. The same methodology was applied in binding assays with SB 242784. We detected binding of bafilomycin A_1 to the selected peptides, while for SB 242784 no interaction took place.

2. Materials

1,2-Dioleoyl-*sn*-glycero-3-phosphoethanolamine-N-(7-nitro-2-1,3-benzoxadiazol-4-yl) (NBD-DOPE), 1,2-Dioleoyl-*sn*-glycero-3-phosphocholine (DOPC), 1,2-Dioleoyl-*sn*-glycero-3-[Phospho-rac-(1-glycerol)] (DOPG), 1,2-Dierucoyl-*sn*-glycero-3-phosphocholine (DEuPC), 2-Lauroyl-*sn*-glycero-3-phosphocholine (DLPC) and 1,2-Miristoyl-*sn*-glycero-3-phosphocholine (DMPC) were obtained from Avanti Polar Lipids (Birmingham, AL). (2Z,4E)-5-(5,6-dichloro-2-indolyl)-2-methoxy-N-(1,2,2,6,6-pentamethylpiperidin-4-yl)-2,4-pentadienamide (SB 242784) was synthesized as described elsewhere [22]. Bafilomycin A_1 was obtained from LC Laboratories (Woburn, MA). Peptides H4, $H4_{A\leftarrow E}$, and H4c′ (see Fig. 2) were synthesized by Pepceuticals (Nottingham, UK). Trifluoroacetic acid (TFA), 16-DOXYL-stearic acid (2-(14-Carboxytetradecyl)-2-ethyl-4,4-dimethyl-3-oxazolidinyloxy) and 5-DOXYL-stearic acid (2-(3-Carboxypropyl)-4,4-dimethyl-2-tridecyl-3-oxazolidinyloxy) were obtained from Sigma-Aldrich (St. Louis, USA). Trifluoroethanol (TFE) was obtained from Acrōs Organics (Geel, Belgium). Other fine chemicals were obtained from Merck (Darmstadt, Germany).

3. Experimental procedures

3.1. Sample preparation

The peptides (Fig. 2) were solubilized in 100 μl of TFA and immediately dried under a $N_{2(g)}$ flow. Following that, the peptide was suspended in TFE. When the TFA solubilization step was not introduced, the solubility in TFE was greatly reduced, and the peptide aggregation levels after reconstitution in lipid bilayers were enhanced.

For peptide reconstitution in lipid bilayers, the desired amount of phospholipids and solubilized peptide (and of the inhibitors in the inhibitor binding studies) were mixed in chloroform and dried under a $N_{2(g)}$ flow. The sample was then kept in vacuum overnight. Liposomes were prepared with buffer Tris 10 mM pH 7.4. The hydration step was performed with gentle addition of buffer at a temperature above the phospholipid main transition temperature.

For the fluorescence quenching experiments with the N-DOXYL-stearic acids, the nitroxide labeled fatty acids were 10% of the total lipid (molar fraction).

3.2. CD measurements

CD spectroscopy was performed on a Jasco J-720 spectropolarimeter with a 450 W Xe lamp. Samples for CD spectroscopy were extruded 8 times on a homemade extruder using polycarbonate filters of 0.1 μm. Peptide concentration was always 40 μM.

3.3. Fluorescence spectroscopy

Steady-state fluorescence measurements were carried out with an SLM-Aminco 8100 Series 2 spectrofluorimeter (with double excitation and emission monochromators, MC400) in a right angle geometry. The light source was a 450 W Xe arc lamp and for reference a Rhodamine B quantum counter solution was used. Correction of emission spectra was performed using the correction software of the apparatus. 5×5 mm quartz cuvettes were used. All measurements were performed at room temperature.

The emission spectrum from the tyrosine of peptide H4 was recorded using an excitation wavelength of 270 nm. The tyrosine quantum yield of peptide H4 in lipid bilayers was determined using quinine sulfate (ϕ=0.55) as a reference [28].

4. Results

4.1. Characterization of reconstituted peptides

When using a peptide as a model for a protein section, it is important that it retains the structural properties of the latter [21]. Therefore, it was important for the present study to accurately know the behavior of the peptides when incorporated in lipid bilayers. The characterization focused on secondary structure, aggregation and position in the bilayer. The 4th transmembrane segment from which the peptide is derived is expected to assume a α-helical structure inside the V-ATPase subunit c, and therefore conditions that favor this type of structure should be determined and used throughout the study.

CD spectra of peptide H4 incorporated in DOPC at a lipid to protein ratio (L/P-molar ratio) of 50 revealed the presence of different types of secondary structures (Fig. 3). Deconvolution of the spectrum with the CDNN CD Spectra Deconvolution v. 2.1 software recovered a fraction of about 40% of α-helical structure, 29% was reported to be random coil, while the remaining was divided between the different types of β-sheet structure. When a L/P ratio of 25 was used, the fraction of α-helical structure present decreased to 30.5%. The presence of increasing amounts of β-sheet structure at lower L/P ratios is an indication of peptide aggregation [29]. It was not possible to obtain a reasonable quality CD spectrum with samples of larger L/P ratios as those used in the inhibitor binding studies, as the lipid concentration became too high and large light scattering problems arose.

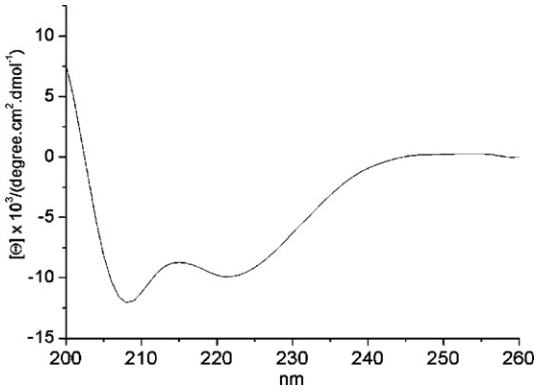

Fig. 3. CD spectrum of peptide H4 incorporated in DOPC at an L/P of 50.

Another method to study aggregation of peptides is to follow the quantum yield changes of the aromatic residues present. Fluorescence from tyrosine residues is known to be quenched by several mechanisms besides FRET, namely interactions with other residues side chains such as glutamate and aspartate, and uncharged forms of basic residues such as arginine, lysine and histidine, as well as electron transfer to peptide α-carbonyl groups [30,31]. Considering this, it can be expected that peptides forming aggregates will have a lower quantum yield than their monomeric counterparts. The quantum yield dependence of Tyr15 (corresponding to Tyr142 in the native protein [32]) from reconstituted peptides on the lipid composition is shown in Fig. 4. The presence of anionic phospholipids clearly increases the quantum yield of peptide H4. In liposome of pure zwitterionic phospholipids, the Tyr15 quantum yield trend is: DEuPC< DOPC<DMPC<DLPC. This difference was not a peptide partition effect because the use of larger lipid concentrations while keeping the same lipid to protein ratio did not result in increased Tyr15 quantum yields. This was expected from the high hydrophobic character of the peptide. On the basis of the higher quantum yield, the anionic lipids seem to be a better choice i.e., the protein fraction in the monomeric form is larger. However, it is necessary to check if the peptide in this type of membranes is in the desired transmembrane configuration, or if it is adsorbed at the interface. This can be determined from differential quenching data, as described below.

The Tyr15 transverse positions relative to the center of the bilayer, obtained by the parallax method [33] using fatty acids labeled with a nitroxide at different depths, are also presented in Fig. 4. In the presence of anionic phospholipids, the peptides adopt a more superficial position in the bilayer (8–11 Å from the center of the bilayer). It is probable that a population of peptide H4 remains in a transmembrane orientation while another adopts a superficial location. A similar situation should be taking place when long chain lipids are used (DEuPC), as the position recovered for Tyr15 (9 Å) is also more superficial than in the other pure zwitterionic phospholipids (around 6 Å) and no significant difference is observed between saturated (DMPC) and unsaturated (DOPC) phosphatidylcholines of similar acyl chain lengths. This Tyr15 position is in agreement with a scenario where peptide H4 is in a transmembrane orientation, as this aromatic residue is only slightly displaced from the center of the peptide sequence. The displacement to a more superficial location of the Tyr15 when different lipids were used (DOPG or DEuPC), is also in agreement with a transmembrane orientation of the peptides in DOPC.

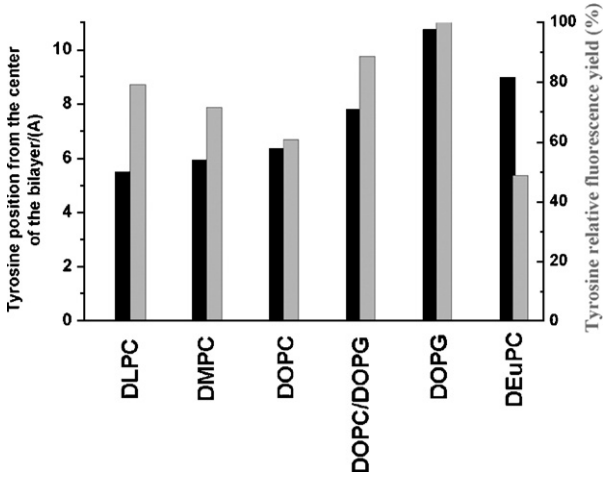

Fig. 4. Position of the Tyr15 residue of peptide H4 as determined by the parallax method (dark bars) and relative fluorescence quantum yield of Tyr15 (light bars) for the peptide incorporated in different lipid systems at an L/P of 100.

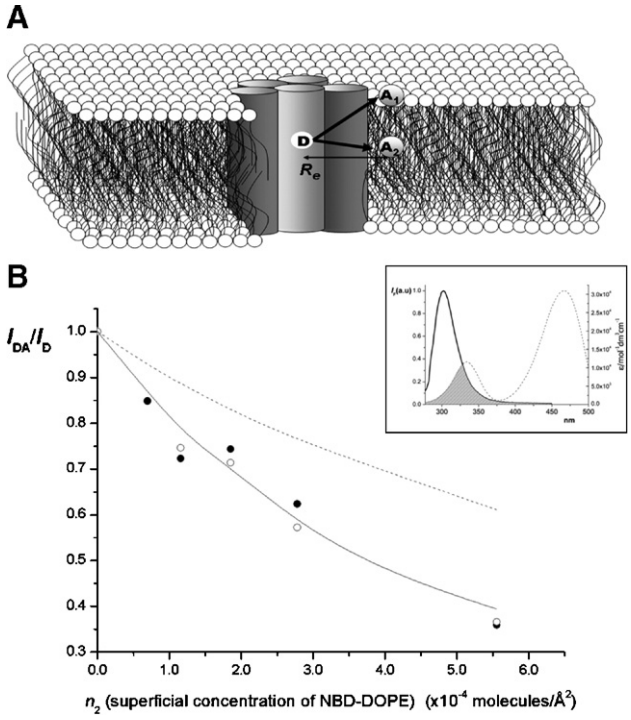

Fig. 5. (A): Model used for FRET simulations. The donor (Tyr15) is located 6 Å from the center of the bilayer while the acceptors can be located at different planes, assuming a superficial location such as for NBD-DOPE (A_1) or more buried positions such as for the V-ATPase inhibitors (A_2). In case of aggregation the number of protein–protein contacts increases while protein–lipid contacts decrease, as a result, R_e (exclusion distance) increases. (B) H4 fluorescence quenching of Tyr15 of peptide H4 due to FRET to NBD-DOPE in DOPC bilayers using a lipid to protein ratio of 50 (●) and 100 (○). Curve corresponds to an exclusion radius fit to the energy transfer data using equations 1–5 (—). A value of 9 Å was recovered for R_e. (– – –) FRET simulation for a random distribution of acceptors around a donor with an exclusion radius of 20 Å. n_2 is the superficial concentration of labeled phospholipids (molecules per Å^2). The range of NBD labeled phospholipid to total phospholipid ratios in this experiment was 0.4% to 2%. Inset: Overlap between tyrosine fluorescence emission (—) and DOPE-NBD absorption spectrum (– –), $R_{0\ (Tyr\text{-}NBD)}$=22 Å.

On the basis of these results, the lipid composition chosen for the inhibitor-peptide binding studies by FRET measurements was 100% DOPC at an L/P of 100, as this lipid is able to favor the transmembrane orientation for peptide H4. The problem of lateral aggregation in the membrane nevertheless potentially remained, as in DOPC the tyrosine quantum yield was significantly lower than in liposomes containing anionic phospholipids. The possibility of aggregation could however also be assessed, as described below.

A FRET experiment was performed in order to determine the size of the possible aggregates. Using the Tyr15 as a donor and NBD labeled DOPE as acceptors (NBD-DOPE), FRET efficiencies were obtained (Fig. 5B). Fitting the available theoretical models for energy transfer between donor and acceptors in different planes [34] to our experimental data, we can recover an averaged exclusion radius (R_e) of the donor, defined as the minimum distance between the Tyr15 and the NBD labeled phospholipids (Fig. 5A). For a monomeric peptide this value should be around 10 Å as this is approximately the sum of the radius of a α-helix backbone and that of a phospholipid molecule. Any significant increase from this value is likely to be reporting an extensive aggregation phenomenon.

FRET efficiencies (E) are calculated from the degree of fluorescence emission quenching of the donor caused by the presence of acceptors.

$$E = 1 - \frac{I_{DA}}{I_D} = 1 - \int_0^\infty i_{DA}(t)\mathrm{d}t \Big/ \int_0^\infty i_D(t)\mathrm{d}t \tag{1}$$

$$i_{DA}(t) = i_D(t)\cdot\rho_{\text{interplanar}}(t) \tag{2}$$

where I_{DA} and I_D are the steady-state fluorescence intensities of the donor in the presence and absence of acceptors respectively. i_{DA} and i_D are the donor decays in the presence and absence of acceptors. $\rho_{\text{interplanar}}$ is the FRET contribution arising from energy transfer to randomly distributed acceptors in two different planes from the donors (two monolayer leaflets) [34].

$$\rho_{\text{interplanar}} = \exp\left\{-2n_2\pi l_1^2 \int_0^{\frac{l_1}{\sqrt{l_1^2+R_e^2}}} \frac{1-\exp(-tb_1^3\alpha^6)}{\alpha^3}\mathrm{d}\alpha\right\}\exp\left\{-2n_2\pi l_2^2 \int_0^{\frac{l_2}{\sqrt{l_2^2+R_e^2}}} \frac{1-\exp(-tb_2^3\alpha^6)}{\alpha^3}\mathrm{d}\alpha\right\} \tag{3}$$

where $b_i=(R_0^2/l_i)^2\tau_D^{-1/3}$, R_0 is the Förster radius, n_2 is the acceptor density in each leaflet, and l_1 and l_2 are the distance between the plane of the donors and the two planes of acceptors. Using Eqs. (1)–(3), theoretical expectations for FRET efficiency in a random distribution of acceptors can be calculated and converted to I_{DA}/I_D ratios. The Förster radius is given by:

$$R_0 = 0.2108(J\kappa^2 n^{-4}\phi_D)^{1/6} \tag{4}$$

where J is the spectral overlap integral, κ^2 is the orientation factor, n is the refractive index of the medium, and ϕ_D is the donor quantum yield. J is calculated as:

$$J = \int f(\lambda)\varepsilon(\lambda)\lambda^4 d\lambda \tag{5}$$

where $f(\lambda)$ is the normalized emission spectra of the donor and $\varepsilon(\lambda)$ is the absorption spectra of the acceptor. The numeric factor in Eq. (4) assumes nm units for the wavelength λ and Å units for R_0.

Assuming the already determined value for Tyr15 position in the bilayer (6 Å from the center) and the distance from the center of the bilayer of the NBD moiety in NBD labeled phospholipids (19 Å) [35], l_1 and l_2 were determined to be 13 and 25 Å, respectively. Using Eqs. (4) and (5) the Förster radius of the Tyr-NBD donor–acceptor pair was determined to be $R_0=22$ Å. In the fitting procedure, these values are kept fixed and the only parameter being fitted is R_e. The results from the experiment along with the curve fitted from the theoretical model, are presented in Fig. 5B. Both sets of data ($L/P=50$ and 100) were fitted with a value of $R_e=9$ Å, matching the expectation for a monomeric peptide. In case there were aggregates at the protein concentrations used these must be small enough so that the distances between Tyr15 and the surrounding phospholipids are not affected. From Eqs. (1)–(3) and using the same parameter values described above as well as $R_e=20$ Å (large aggregates), a FRET simulation was performed for the same system and the obtained donor quenching curve is compared to our experimental values in Fig. 5B.

4.2. Peptide inhibitor binding studies

Both bafilomycin A_1 and SB 242784 absorb in the UV region and can act as acceptors for tyrosine in energy transfer experiments (spectra are shown in Fig. 6 and 7). The Förster radius for the Tyr-bafilomycin A_1 donor–acceptor pair is 20 Å, whereas for the Tyr-SB 242784 pair it is 24 Å (Eq. (4)). A 3 mM concentration of lipid was used to ensure an almost complete incorporation of inhibitors in the bilayer. SB 242784 partition coefficient to DOPC bilayers is 1.20×10^4 [36], and at the lipid concentration used 97% of the inhibitor molecules are incorporated in the bilayer. The fraction of inhibitors not incorporated in the vesicles was taken into account on the acceptor concentrations plot in Fig. 7, which depicts the Tyr15 quenching via energy transfer to SB 242784.

In contrast to SB 242784, bafilomycin A_1 is not a fluorescent molecule and partition coefficients could not be determined using photophysical techniques. Overestimation of its partition coefficient could lead to an underestimation of bafilomycin-peptide binding constants. However, it was recently showed by EPR of spin-labeled lipids that the macrolide molecule concanamycin A, another powerful V-ATPase inhibitor with very similar structure to bafilomycin A_1, readily incorporates in lipid membranes [37]. Thus, it is to be expected from this result and from the high hydrophobic character of the molecule that the incorporation of bafilomycin A_1 at the lipid concentrations used is close to 100%.

On the inhibitor-peptide binding assays, the L/P was kept at 100 in order to ensure minimum levels of aggregation. Experimental FRET efficiencies obtained with both peptide H4/SB 242784 and peptide H4/bafilomycin A_1 donor/acceptor pairs (Eq. (1)), are compared to theoretical expectations for a random distribution of acceptors (the scenario in which there is an absence of binding) obtained from Eqs. (1) and (2) (see Figs. 6 and 7). The position of SB 242784 in DOPC bilayers was already determined from selective quenching methodology (parallax method) to be 12.8 Å from the center of the bilayer [36], but the position of the bafilomycin A_1 chromophore was impossible to determine by the same methodology since this molecule is not fluorescent. In Fig. 6A, the simulations corresponding to different positions of the bafilomycin A_1 chromophore inside the bilayer are shown, together with the experimental data. It is clear that even when assuming that the Tyr15 is located on the same bilayer plane as the bafilomycin A_1 chromophore (6 Å from the center of the bilayer), in a situation of maximal energy transfer efficiency, the experimental energy transfer efficiencies cannot be solely explained by the unbound population of inhibitor molecules (i.e. random distribution of acceptors) and a fraction of peptide H4 must be binding bafilomycin A_1. It is difficult to precisely quantify the binding constant (K_b) for this process due to the uncertainty relative to the bafilomycin A_1 chromophore position in the bilayer, but a lower and a higher limit can be determined assuming the closest and furthest position possible for bafilomycin A_1 and Tyr15 (corresponding respectively to a position in the center and in the surface of the bilayer for bafilomycin A_1), and also that peptide H4/bafilomycin A_1 complexes are completely non-fluorescent (Eqs. (6) and (7)). This last assumption is valid, since for a contact interaction either by Förster type or other transfer (exchange) mechanism, the efficiency of transfer would be 100%. The equations valid for the FRET efficiency in a scenario of peptide H4-bafilomycin A_1 1:1 complex formation are given below:

$$E_{EXP} = E_{random} + \frac{H4 - Baf}{[H4]_T}(1 - E_{random}) \tag{6}$$

$$\frac{[H4-Baf]}{[H4]_T}=\frac{-1-K_b([Baf]_T+[H4]_T)+\sqrt{(1+K_b([Baf]_T+[H4]_T))^2-4(K_b^2[Baf]_T[H4]_T)}}{(-2K_b)[H4]_T} \quad (7)$$

where [*H4-Baf*] is the effective concentration (molecules per lipid volume as the binding is confined to the lipid phase) of the peptide–bafilomycin A_1 complex, and, $[H4]_T$ and $[Baf]_T$ are respectively, the effective analytical concentrations of the peptide and of bafilomycin A_1. E_{EXP} is the energy transfer efficiencies obtained experimentally and E_{random} is the theoretical energy transfer efficiency assuming a random distribution of acceptors (Eqs. (1)–(3)). In case binding is detected, the use of effective bafilomycin A_1 concentrations will result in lower binding constants as compared to the ones of bulk concentrations, but the binding constants obtained in this way have a larger physical meaning as they will not change with lipid concentration. Anyway they can be easily interconverted.

Assuming a position for bafilomycin A_1 in the center of the bilayer, the fitting procedure (Fig. 6A) recovered $K_b = 10.5 \pm 1.32\ M^{-1}$ (mol per volume of lipid). When the bafilomycin A_1 position was fixed to 20 Å from the center of the bilayer (i.e. at the surface), the value recovered was $K_b = 36.2 \pm 2.8\ M^{-1}$. Therefore, the binding constant upper and lower bounds for the peptide H4–bafilomycin A_1 complex are $10.5 \pm 1.32 < K_b < 36.2 \pm 2.8\ M^{-1}$. However, it is to be expected that, due to the hydrophobic character of the bafilomycin A_1 molecule, the real value should be located near the lower limit of this interval.

The same experiment was performed using peptides $H4_{A \leftarrow E}$ and H4c′ (Fig. 2)). In peptide $H4_{A \leftarrow E}$ the glutamate, which corresponds to the natural amino acid expected to play a key role in the proton translocation process, was changed to an alanine, and peptide H4c′ corresponds to the 4th transmembrane helix of the c′ isoform of the c-subunit. Both peptides were characterized in DOPC with identical results to peptide H4. The results for the inhibitor binding assays are shown in Fig. 6B. The recovered lower bounds for the binding constants were: $K_b(H4_{A \leftarrow E}) > 20.6 \pm 4.46\ M^{-1}$ and $K_b(H4c') > 13.72 \pm 3.05\ M^{-1}$.

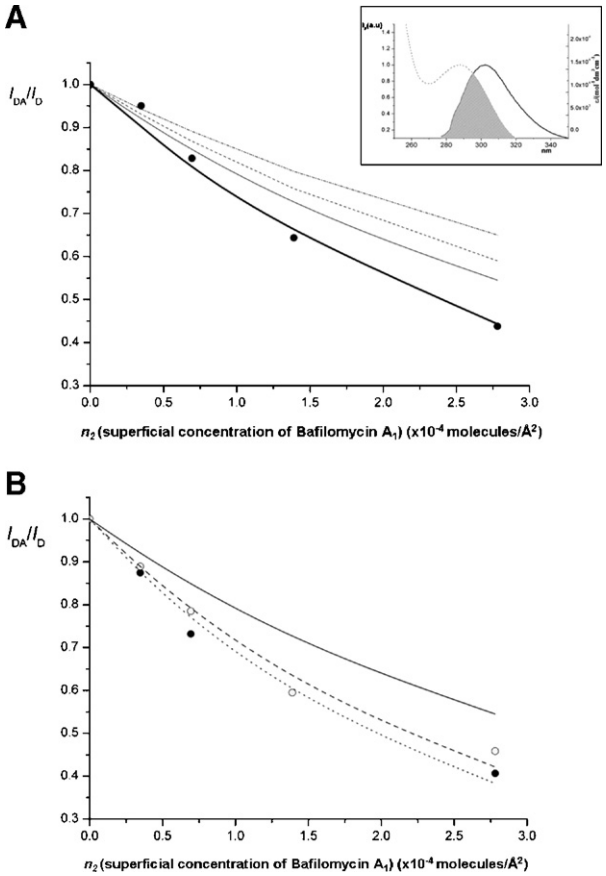

Fig. 6. (A) Fluorescence emission quenching of Tyr15 of peptide H4 by FRET to bafilomycin A_1(●). Theoretical expectations (Eqs. (1–3)) for FRET in the absence of inhibitor binding to peptide H4 assuming positions for bafilomycin A_1 of 12.5 Å (···), 8.5 Å (– – –), and 4.5 Å (—) from the center of the bilayer. (—) Fitting of equations 6 and 7 to FRET data assuming a bafilomycin A_1 position of 4.5 Å from the center of the bilayer. The interval $10.5 \pm 1.34 < K_{b(H4\text{-bafilomycin A1})} < 36.2 \pm 2.78$ was recovered. Inset: Overlap between tyrosine fluorescence emission (—) and bafilomycin A_1 absorption spectrum (– – –), $R_{0\ (Tyr\text{-bafilomycin A1})} = 20$ Å. (B) Fluorescence emission quenching of peptide $H4_{A \leftarrow E}$ (●) and peptide $H4_{c'}$ (○) tyrosine by FRET to bafilomycin A_1. Theoretical expectations (Eqs. (1–3)) for FRET in the absence of inhibitor binding to peptide H4, assuming positions for bafilomycin A_1 of 4.5 Å from the center of the bilayer (—). FRET data fitted to Eqs. 6 and 7 assuming a bafilomycin A_1 position of 4.5 Å from the center of the bilayer. $K_{b(H4A \leftarrow E\text{-bafilomycin A1})} \geq 20.6 \pm 4.46$ (···) and $K_{b(H4c'\text{-bafilomycin A1})} \geq 13.7 \pm 3.05$ (– – –) were recovered. The range of bafilomycin to total phospholipid ratios in these experiments was 0.25% to 2%.

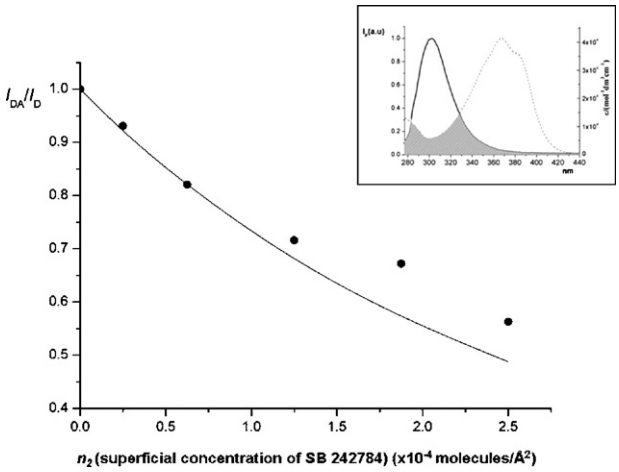

Fig. 7. Fluorescence emission quenching of Tyr15 of peptide H4 by FRET to SB 242784 (●). Curve corresponds to the theoretical expectation for FRET in the absence of inhibitor binding to peptide H4 (see text). The range of SB 242784 to total phospholipid ratios in these experiments was 0.18% to 1.8%. Inset: overlap between tyrosine fluorescence emission (—) and SB242784 absorption spectrum (– – –), R_0 (Tyr-SB 242784)=24 Å.

When the FRET binding assay was applied to the peptide H4/SB 242784 system, the results were substantially different (Fig. 7). With this inhibitor, the obtained FRET efficiencies matched the theoretical expectations for a random distribution of acceptors, suggesting absence of binding between SB 242784 and the peptide. No uncertainty exists regarding this result as the position of the inhibitor inside the bilayer is accurately know from parallax fluorescence quenching techniques (12.8 Å from the center of the bilayer — [36]).

5. Discussion

5.1. Use of peptide H4 as a model peptide for the 4th transmembrane segment of subunit c

Aggregation of transmembrane peptides containing a hydrophobic sequence and flanked by basic residues has already been reported [38–40], thus detection of aggregates of peptide H4 at low L/P ratios (<50) was not surprising. The c-subunit of V-ATPase is expected to be composed of 4 putative transmembrane segments tightly packed between themselves as well as with other transmembrane segments from neighboring subunits inside a hexamer. This preference for protein–protein interactions as opposed to protein–lipid interactions is possibly what drives the detected association between the H4 peptides incorporated in liposomes as detected by CD spectroscopy at low L/P ratios. However, at the higher L/P ratios allowed by fluorescence spectroscopy, the presence of large aggregates can be excluded as the average exclusion radius of the peptide recovered from the data in Fig. 5B, is identical to the expectation for monomeric species. It is clear from Fig. 5B that a scenario where R_e is significantly larger than 10 Å (as expected for large aggregates) is not compatible with our results further validating our conclusions.

It could be invoked that due to null or very low Tyr15 quantum yields of aggregated H4 peptides, the fraction of donor light from aggregated species is negligible and the fraction of fluorescence from monomeric peptides is largely dominant. In such a case, the obtained FRET efficiencies only concern monomeric peptides as donors and the fluorescence data from FRET binding measurements to V-ATPase inhibitors would not be affected by a population of aggregated peptides with low exposure to bulk phospholipids in which the inhibitors binding sites could be occluded. In both cases, we can expect that the peptides containing unquenched tyrosines are exposed to the lipid environment, ensuring accessibility towards inhibitors and feasibility of the inhibitor binding assays (the lipid exposure of a surface of the 4th transmembrane segment is in fact expected in the intact c subunit [7,10]). From all of the above evidence, we expect that peptide aggregation under our experimental conditions is not biasing the data.

5.2. Inhibitor/Peptide FRET binding assays

The mechanism of inhibition of V-ATPase by macrolide inhibitors as well as by synthetic molecules has recently been the target of extensive study and debate [8,9,26,27]. It is still not clear which domains of the enzyme contribute to the formation of the inhibitors binding site. Bowman and coworkers identified several mutations in the V-ATPase able to completely disrupt bafilomycin A_1 inhibitory activity, all of these located in the c-subunit and the majority of them in the domain expected to comprise the 4th transmembrane segment [5,9]. From FRET measurements, it was shown that concanamycin and SB 242784 bound competitively to the c-subunit, clearly suggesting an overlap of the inhibitor binding sites [27]. The dissociation constants of the protein–inhibitor complex were also relatively close to the published IC_{50} values for SB 242784. Therefore, it seems that all structural requirements for inhibitor binding to the membrane bound domain of the V-ATPase are located in the c-subunits, even if particular domains in the a-subunit can play a role in the inhibitory mechanism as proposed by some authors

[26]. In the same way, c-subunit residues shown to be important for bafilomycin A_1 inhibitory activity through mutational studies [9] could not be directly involved in the binding of the inhibitor, but still play a role in the inhibition mechanism. Here, we proposed to further define the structural requirements for bafilomycin A_1 and SB 242784 binding to the V-ATPase, by focusing on the protein domain expected to be the primary contributor to the inhibitor binding site, the putative 4th transmembrane domain of the c-subunit. The extent of binding efficiencies achieved using only peptides corresponding to this section of the protein is an indicator of the relevance of the remaining protein domains to the binding of inhibitor, the first step in the inhibitory mechanism.

No evidence was found supporting SB 242784 association with the peptide H4. On the other hand, bafilomycin A_1 was shown to possess only moderate affinity for the transmembrane peptides. Due to uncertainties in bafilomycin A_1 position in bilayers it was impossible to rigorously quantify a binding constant for the process, but a reliable range for this parameter could be presented. The differences in bafilomycin A_1 binding efficiencies for the peptide H4, H4c′ and $H4_{A\leftarrow E}$ are not significant as they fall within, or close to the error of the fits. For H4c′ this result is somewhat surprising. Mutations on conserved residues of the c-subunit known to confer resistance to bafilomycin A_1 and concanamycin were shown to be ineffective in the c′ and c′ isoforms [9]. It was proposed that if a bafilomycin A_1 binding site was present on these isoforms, then it must possess lower affinity than in the c isoform [9]. If this is the case, then the differences in binding efficiencies between the two isoforms must be explained by discrepancies in the interaction of the inhibitor with parts of the protein other than the highly conserved putative 4th transmembrane helix.

Although the contribution from the 4th transmembrane segment (TM4) to the binding site affinity for bafilomycin A_1 is not negligible, it is absolutely unable to explain the extremely low IC_{50} of bafilomycin A_1 (0.1 nM). The binding efficiencies observed for concanamycin (IC_{50} close to bafilomycin A_1) and the intact isolated c-subunit [27] were more than 1000 times larger than the ones recovered in the present study. Therefore, it is clear that either: (i) the other transmembrane segments from the c-subunit, namely TM1 and TM2, are essential in the formation of an efficient inhibitor binding site, or that (ii) interactions of TM4 with other protein segments are required for this protein section to assume the appropriate folding which enables the establishment of the necessary interactions for an efficient binding between the residues of the 4th transmembrane segment of the c-subunit and the inhibitors. Absence of SB 242784 binding to the peptide H4 could be explained by the much lower IC_{50} of this inhibitor (26 nM in chicken osteoclasts [22]) that reflects a much lower binding site affinity for this inhibitor, and the absence of remaining c-subunit transmembrane segments potentiates this effect.

In this work, in addition to the detailed comparison of the different inhibitors and peptides, it was concluded that in contrast to some reported cases [11–16], there is a very significant difference in binding when comparing the binding to selected protein segments or to the whole protein. Although studies using peptides are very relevant, clearly in the case of the interaction between the bafilomycin A_1 or SB 242784 with the c-subunit from V-ATPase, the whole protein architecture and the environment that it provides, are key factors for an efficient binding.

Acknowledgments

This work was supported by contract no. QLG-CT-2000-01801 of the European Commission (MIVase consortium). M. H. and M. P. are members of the COST D22 Action of the European Union. F. F. acknowledges grant SFRH/BD/14282/2003 from FCT (Portugal). This work was partially funded by FCT (Portugal) under the program POCTI.

References

[1] M.E. Finbow, M.A. Harrison, The vacuolar H+-ATPase: a universal proton-pump of eukaryotes, Biochem. J. 324 (1997) 697–712.
[2] T. Nishi, M. Forgac, The vacuolar (H+)-ATPases—Nature's most versatile proton pumps, Mol. Cell. Biol. 3 (2002) 94–103.
[3] B. Powell, L.A. Graham, T.H. Stevens, Molecular characterization of the yeast vacuolar H+-ATPase proton pore, J. Biol. Chem. 275 (2000) 23654–23660.
[4] M.A. Harrison, M.E. Finbow, J.B. Findlay, Postulate for the molecular mechanism of the vacuolar H(+)-ATPase (hypothesis), Mol. Membr. Biol. 14 (1997) 1–3.
[5] B.J. Bowman, E.J. Bowman, Mutations in subunit c of the vacuolar ATPase confer resistance to bafilomycin and identify a conserved antibiotic binding site, J. Biol. Chem. 277 (2002) 3965–3972.
[6] G. Werner, H. Hagenmaier, H. Drautz, A. Baumgartner, H. Zähner, Metabolic products of microorganisms. Bafilomycins, isolation, chemical structure and biological activity, J. Antibiot. 37 (1984) 110–117.
[7] M. Harrison, B. Powell, M.E. Finbow, J.B.C. Findlay, Identification of lipid-accessible sites on the Nephrops 16-kDa proteolipid incorporated into a hybrid vacuolar H+-ATPase: site-directed labeling with n-(1-pyrenyl) cyclohexylcarbodiimide and fluorescence quenching analysis, Biochemistry 39 (2000) 7531–7537.
[8] T. Páli, G. Whyteside, N. Dixon, T. Kee, S. Ball, M.A. Harrison, J.B.C. Findlay, M.E. Finbow, D. Marsh, Interaction of inhibitors of the vacuolar H+-ATPase with the transmembrane Vo-sector, Biochemistry 43 (2004) 12297–12305.
[9] E.J. Bowman, L.A. Graham, T.H. Stevens, B.J. Bowman, The bafilomycin/concanamycin binding site in subunit c of the V-ATPases from *Neurospora crassa* and *Saccharomyces cerevisiae*, J. Biol. Chem. 279 (2004) 33131–33138.
[10] M. Harrison, J. Murray, B. Powell, Y. Kim, M.E. Finbow, J.B.C. Findlay, Helical interactions and membrane disposition of the 16-kDa proteolipid subunit of the vacuolar H1-ATPase analyzed by cysteine replacement mutagenesis, J. Biol. Chem. 274 (1999) 25461–25470.
[11] T.L. Lentz, V. Chaturverdi, B.M. Conti-Fine, Amino acids within residues 181–200 of the nicotinic acetylcholine receptor alpha 1 subunit in nicotine binding, Biochem. Pharmacol. 55 (1998) 341–347.
[12] P.T. Wilson, T.L. Lentz, E. Hawrot, Determination of the primary amino acid sequence specifying the alpha-bungarotoxin binding site on the alpha subunit of the acetylcholine receptor from *Torpedo californica*, Proc. Natl. Acad. Sci. U. S. A. 82 (1985) 8790–8794.
[13] D. Neumann, D. Barchan, M. Fridkint, S. Fuchs, Analysis of ligand binding to the synthetic dodecapeptide of the acetylcholine receptor a subunit, Proc. Natl. Acad. Sci. U. S. A. 83 (1986) 9250–9253.
[14] A.H. Taylor, G. Heavner, M. Nedelman, D. Sherris, E. Brunt, D. Knight, J. Ghrayeb, Lipopolysaccharide (LPS) neutralizing peptides reveal a lipid A binding site of LPS binding protein, J. Biol. Chem. 270 (1995) 17934–17938.

[15] C. Ried, C. Wahl, T. Miethke, G. Wellnhofer, C. Landgraf, J. Schneider-Mergener, A. Hoess, High affinity endotoxin-binding and neutralizing peptides based on the crystal structure of recombinant Limulus anti-lipopolysaccharide factor, J. Biol. Chem. 271 (1996) 28120–28127.
[16] A.C. Scatigno, S.S. Garrido, R. Marchetto, A 4.2 kDa synthetic peptide as a potential probe to evaluate the antibacterial activity of coumarin drugs, J. Peptide Sci. 10 (2004) 566–577.
[17] S.R. George, G.Y.K. Ng, S.P. Lee, T. Fan, G. Varghese, C. Wang, C.M. Deber, P. Seeman, B.F. O'Dowd, Blockade of G protein-coupled receptors and the dopamine transporter by a transmembrane domain peptide: novel strategy for functional inhibition of membrane proteins in vivo, J. Pharmacol. Exp. Ther. 307 (2003) 481–489.
[18] J.L. Popot, J. Trewhella, D.M. Engelman, Reformation of crystalline purple membrane from purified bacteriorhodopsin fragments, EMBO J. (1986) 3039–3044.
[19] T. Marti, Refolding of bacteriorhodopsin from expressed polypeptide fragments, J. Biol. Chem. 273 (1998) 9312–9322.
[20] S. Ozawa, R. Hayashi, A. Masuda, T. Iio, S. Takahashi, Reconstitution of bacteriorhodopsin from a mixture of a proteinase V8 fragment and two synthetic peptides, Biochim. Biophys. Acta 1323 (1997) 145–153.
[21] R.W. Hesselink, R.B.M. Koehorst, P.V. Nazarov, M.A. Hemminga, Membrane-bound peptides mimicking transmembrane Vph1p helix 7 of yeast V-ATPase: a spectroscopic and polarity mismatch study, Biochim. Biophys. Acta 1716 (2005) 137–145.
[22] G. Nadler, M. Morvan, I. Delimoge, P. Belfiore, A. Zocchetti, I. James, D. Zembryki, E. Lee-Rycakzewski, C. Parini, E. Consolandi, S. Gagliardi, C. Farina, (2Z,4E)-5-(5,6-dichloro-2-indolyl)-2-methoxy-n-(1,2,2,6,6-pentamethylpiperidin-4-yl)-2,4-pentadienamide, a novel, potent and selective inhibitor of the osteoclast V-ATPase, Bioorg. Med. Chem. Lett. 8 (1998) 3621–3626.
[23] S. Gagliardi, G. Nadler, E. Consolandi, C. Parini, M. Morvan, M.N. Legave, P. Belfiore, A. Zocchetti, G.D. Clarke, I. James, P. Nambi, M. Gowen, C. Farina, 5-(5,6-Dichloro-2-indolyl)-2-methoxy-2,4-pentadienamides: novel and selective inhibitors of the vacuolar H+-ATPase of osteoclasts with bone antiresorptive activity, J. Med. Chem. 41 (1998) 1568–1573.
[24] L. Visentin, L.A. Dodds, M. Valente, P. Misiano, J.N. Bradbeer, S. Oneta, X. Liang, M. Gowen, C. Farina, A selective inhibitor of the osteoclastic V-H+-ATPase prevents bone loss in both thyroparathyroidectomized and ovariectomized rats, J. Clin. Invest. 103 (2000) 309–318.
[25] M.F. Manolson, H. Yu, W. Chen, Y. Yao, K. Li, R.L. Lees, J.N.M. Heersche, The a3 isoform of the 100-kDa V-ATPase subunit is highly but differentially expressed in large (10 nuclei) and small (5 Nuclei) osteoclasts, J. Biol. Chem. 278 (2003) 49271–49278.
[26] Y. Wang, T. Inoue, M. Forgac, Subunit a of the yeast V-ATPase participates in binding of bafilomycin, J. Biol. Chem. 280 (2005) 40481–40488.
[27] G. Whyteside, P.J. Meek, S.K. Ball, N. Dixon, M.E. Finbow, T.P. Kee, J.B.C. Findlay, M.A. Harrison, Concanamycin and indolyl pentadieneamide inhibitors of the vacuolar H+-ATPase bind with high affinity to the purified proteolipid subunit of the membrane domain, Biochemistry 44 (2005) 15024–15031.
[28] D.F. Eaton, Reference materials for fluorescence measurement, Pure Appl. Chem. 60 (1988) 1107–1114.
[29] R. Cerpa, F.E. Cohen, I.D. Kuntz, Conformational switching in designed peptides: the helix/sheet transition, Fold. Des. 1 (1996) 91–101.
[30] R.W. Cogwill, Tyrosil fluorescence in proteins and model peptides, in: R.F. Chen, H. Edelhoch (Eds.), Biochemical Fluorescence: Concepts 2, Marcel Dekker, New York, 1976, pp. 441–486.
[31] J.W. Longworth, Excited states of proteins and nucleic acid, in: R.F. Steiner, I. Weinryb (Eds.), Plenum Press, New York, 1971, pp. 319–484.
[32] H. Nelson, N. Nelson, The progenitor of ATP synthases was closely related to the current vacuolar H+-ATPase, FEBS Lett. 247 (1989) 147–153.
[33] A. Chattopadhyay, E. London, Parallax method for direct measurement of membrane penetration depth utilizing fluorescence quenching by spin-labeled phospholipids, Biochemistry 26 (1987) 39–45.
[34] L. Davenport, R.E. Dale, R.H. Bisby, R.B. Cundall, Transverse location of the fluorescent probe 1,6-diphenyl-1,3,5-hexatriene in model lipid bilayer membrane systems by resonance energy transfer, Biochemistry 24 (1985) 4097–4108.
[35] F.S. Abrams, E. London, Extension of the parallax analysis of membrane penetration depth to the polar region of model membranes: use of fluorescence quenching by a spin-label attached to the phospholipid polar headgroup, Biochemistry 32 (1993) 10826–10831.
[36] F. Fernandes, L. Loura, R.B.M. Koehorst, N. Dixon, T.P. Kee, M.A. Hemminga, M. Prieto, Interaction of the indole class of V-ATPase inhibitors with lipid bilayers, Biochemistry 45 (2006) 5271–5279.
[37] T. Páli, N. Dixon, T.P. Kee, D. Marsh, Incorporation of the V-ATPase inhibitors concanamycin and indole pentadiene in lipid membranes, Spin-label EPR studies, Biochim. Biophys. Acta 1663 (2004) 14–18.
[38] J. Ren, S. Lew, J. Wang, E. London, Control of the transmembrane orientation and interhelical interactions within membranes by hydrophobic helix length, Biochemistry 38 (1999) 5905–5912.
[39] F.X. Zhou, H.J. Merianos, A.T. Brunger, D.M. Engelman, Polar residues drive association of polyleucine transmembrane helices, Proc. Natl. Acad. Sci. U. S. A. 98 (2000) 2250–2255.
[40] S. Mall, R. Broadbridge, R.P. Sharma, J.M. East, A.G. Lee, Self-association of model transmembrane helix is modulated by lipid structure, Biochemistry 40 (2000) 12379–12386.